Structure, crystallization and morphology of poly(aryl ether ketone ketone)*

KennCorwin H. Gardner†‡, Benjamin S. Hsiao§, Robert R. Matheson Jr‡ and Barbara A. Wood‖

Central Research and Development, Fibers and Polymers, E.I. DuPont de Nemours, Experimental Station, Wilmington, Delaware 19880-0356, USA

The structure, crystallization and morphology of poly(aryl ether ketone ketone)s (PEKKs) prepared from diphenyl ether (DPE), terephthalic acid (T) and isophthalic acid (I) and having different T/I ratios have been investigated. As prepared, these copolymers can be thought of as consisting of 'phthalate diads' containing –DPE–T–DPE–T– (TT) and/or –DPE–T–DPE–I– (TI). Melt-crystallized PEKKs (all T/I ratios) form a structure similar to that observed in other poly(aryl ether ketone)s (form 1; $a = 0.769$ nm, $b = 0.606$ nm and fibre axis $c = 1.016$ nm). However, depending on composition, both TT and TI crystals were observed. All PEKK materials grow in the form of spherulites having negative birefringence. The incorporation of isophthaloyl moieties is observed to increase the chain flexibility and decrease the rate of crystallization. The equilibrium melting temperatures of various PEKKs were estimated using the Hoffman–Weeks approach, and showed a linear correlation with the *meta* isomer content. In contrast to other poly(aryl ether ketone)s, a form 2 crystalline modification ($a = 0.393$ nm, $b = 0.575$ nm and $c = 1.016$ nm) can be induced either by exposure to solvents or by cold crystallization. The two crystalline modifications differ from each other in the placement of the chains and, consequently, the interchain interactions.

(Keywords: poly(ether ketone ketone); structure; crystallization; morphology; copolymer; X-ray diffraction; thermal analysis; electron microscopy)

INTRODUCTION

High-temperature, high-performance thermoplastic poly(aryl ether ketone)s are of scientific interest. The chemical structure and linkage composition of some members of the poly(aryl ether ketone) family are given in *Table 1*. These polymers are members of a family that can be schematically represented as –P–Li– where P is a 1,4- or 1,3-linked phenyl group and Li signifies either an ether or a keto linkage. The effect of keto content on the crystallization of poly(aryl ether ketone)s has been discussed[1–4]. Ether linkages have a relatively shallow rotational conformation energy barrier and thus are more flexible than a keto linkage[5]. The addition of keto linkages inevitably increases the stiffness of the molecule, as reflected by the increase of glass temperature[6]. An increase of keto linkages also enhances the packing efficiency of the unit-cell structure, thereby producing a larger crystal binding (or cohesive) energy or a higher melting temperature[1] (*Figure 1*). Powder diffraction patterns of three family members are shown in *Figure 2*. The diffraction patterns for poly(aryl ether ether ketone) (PEEK), poly(aryl ether ketone) (PEK) and poly(aryl ether ketone ketone) (PEKK(T/I = 100/0)), all crystallized from the melt, are similar in kind but exhibit a small shift in peak positions to lower angle with increase in keto content. This shift is reflected in the systematic changes in the unit-cell parameters (*Figure 3*). The crystalline structures of poly(phenylene oxide) (PPO), PEK and PEEK have been previously described[1–4,7–11].

The poly(aryl ether ketone) that has previously received the most attention is poly(aryl ether ether ketone). PEEK can be crystallized from dilute solution, from the melt, or from quenched samples exposed to low-molecular-weight solvents. Solution-crystallized PEEK has recently been studied by Lovinger *et al.*[12]. They concluded that similar morphologies were found for solution-crystallized and melt-crystallized specimens[13–17]. Both routes produce spherulites with narrow, elongated lamellae, that grow radially in the crystallographic *b*-axis direction. In this structure, the *c* axis lies parallel to the spherulite plane and the *a* axis lies vertical to the plane. Since the anisotropy of polarizability of a PEEK chain is positive ($a_c > a_b$)[16], the above molecular arrangement should produce a negative birefringence in spherulites. This is consistent with many experimental observations[13,16]. The morphology of melt-crystallized PEEK specimens depends strongly on the thermal history, the molecular weight and the degree of crosslinking[13–17]. This behaviour is similar to that of other semicrystalline polymers. PEEK exhibits a lower degree of crystallinity (less than ca. 40%) than polymers such as polyethylene or polyoxymethylene, possibly due to the high rigidity of the chain[18].
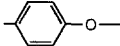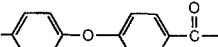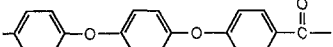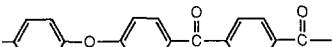
Table 1 Chemical structures of members of the poly(aryl ether ketone) family and their keto contents

Structure	Name	Ketone (%)
	PPO	0
	PEK	50
	PEEK	33
	PEKK	67

In this work, we discuss some general aspects of the crystallization and morphology of PEKKs having different T/I ratios. Two issues will be addressed. One is the characterization of the two crystal structures. Another is the effect of T/I ratio on features of the crystallization behaviour such as melting temperature, double-melting behaviour, crystallization kinetics and recrystallization. This work is based on X-ray diffraction and thermal analysis studies. Morphology will be discussed in terms of the spherulitic structure obtained from the melt as revealed by electron microscopy following permanganic etching, optical microscopy and small-angle light scattering. The thermal history effect on the morphology will also be discussed.

Figure 1 Plot of transition temperatures vs. keto content. The full symbols represent transition temperatures for all-*para* poly(aryl ether ketone)s taken from the literature. The open symbols represent transition temperatures for PEKK samples with different T/I ratios

EXPERIMENTAL

Materials and preparation

PEKK samples used were developmental grade polymers made by Du Pont. The polymers were prepared from diphenyl ether (DPE), terephthalic acid (T) and isophthalic acid (I) in a two-step process and have a generalized chemical structure as follows, but differ from each other by their *para/meta* phenyl isomer ratios, i.e.

Non-crystalline PEEK specimens can be crystallized by exposure to interactive solvents such as methylene chloride[19-23]. The presence of solvents increases chain mobility and so facilitates crystallization. The crystalline phase observed in solvent-crystallized PEEK is apparently identical to that derived from melt or solution[19-23].

A unique member of the high-performance poly(aryl ether ketone) family is poly(aryl ether ketone ketone)[22-26]. PEKK, which is prepared from diphenyl ether (DPE), terephthalic acid (T) and isophthalic acid (I), has a higher percentage of keto linkages (67%) than other poly(aryl ether ketone)s. The all-*para*-linked polymer (T/I ratio 100/0) has a high glass transition temperature ($T_g \sim 165°C$), but melts too close to its thermal degradation temperature to be of practical use. By incorporating *meta* linkages into the PEKK structure via the isophthaloyl moieties, the melting temperature can be lowered into a usable range while retaining a high glass temperature (*Figure 1*).
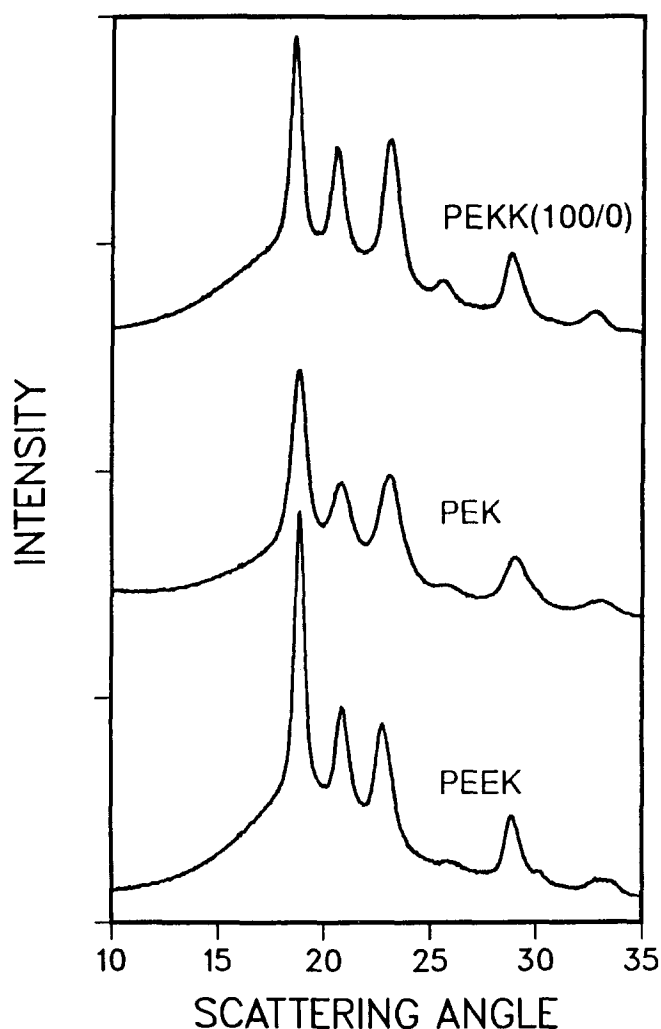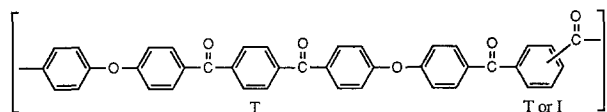
Unlike PEEK, which has a single crystalline modification, PEKK shows two stable crystalline polymorphs: form 1, the conventional structure, and a new structure (form 2) obtained by solvent crystallization or cold crystallization[22,23,27].

Figure 2 X-ray powder diffraction patterns of melt-crystallized PEEK, PEK and PEKK (T/I = 100/0)

T/I ratio:

Six T/I ratios were prepared for this work: 100/0, 90/10, 80/20, 70/30, 60/40 and 50/50. Because of the synthetic route, these polymers can be thought of as copolymers of the 'diads' containing –DPE–T–DPE–T– (TT) and/or –DPE–T–DPE–I– (TI). The polymer compositions, in terms of TT and TI diads, are given in *Table 2*. This point of view makes it apparent that T/I ratios of 100/0 and 50/50 result in homopolymers. In all cases the isophthalate units are separated by a minimum of five phenyl groups.
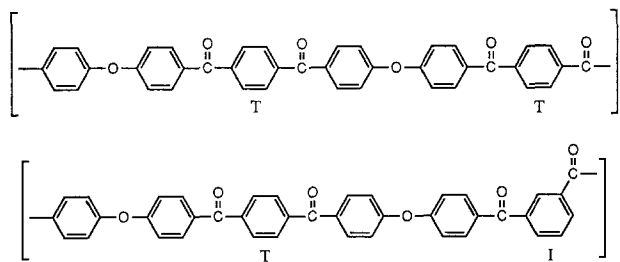
All of the polymers have number-average molecular weights (M_n) and weight-average molecular weights (M_w) of about 100 000 and 30 000, respectively.

Samples were vacuum dried at 120°C for 24 h prior to all experiments. Thin films (ca. 5 μm) for optical microscopy and small-angle light scattering studies were prepared by pressing powder specimens at about 30°C above the melting temperature. Samples for X-ray diffraction experiments, 125 μm thick, were made using this procedure followed by a water quench. Post-treatments to the X-ray samples included exposure to methylene chloride (anhydrous grade), annealing at 200°C, remelting and isothermal crystallization at 200 or 300°C as already reported in a preliminary account[23]. PEKK plaques were prepared under various thermal treatments for transmission electron microscopy (TEM) of surface replicas following permanganic etching. These treatments included slow cooling (about 5°C min^{-1}) and annealing at a high (30°C below T_m) and a low (100°C below T_m) temperature.

The permanganic etching was performed as follows, which is slightly different than that proposed for PEEK[15]. A solution containing 50 ml concentrated sulphuric acid, 30 ml 85% phosphoric acid and 2 g of ground potassium permanganate was prepared and then 10 ml of distilled water was added. The specimen was immersed in this solution for about 1 h in an ultrasonic bath to prevent redeposition of degraded polymer[28]. Recovered specimens were then rinsed with water and air dried. Etched specimens were exposed to a carbon–platinum vapour

at low angle inside a vacuum evaporator, coated with poly(acrylic acid) solution, and allowed to dry. The dry replica was stripped and was vacuum evaporated with carbon. The poly(acrylic acid) coating was dissolved by overnight soaking onto the surface of water in a Petri dish. The remaining replica was picked up on copper mesh grids, dried and transferred to the microscope.

Characterization techniques

X-ray diffraction. X-ray diffractometry scans were collected in the symmetrical transmission mode using an automated Philips diffractometer (curved crystal monochromator, 1° divergence and receiving slits, sample rotating) and Cu Kα radiation. Data were collected in a fixed time mode with a step size of 0.05° and run from $2\theta = 4°$ to 65°. Data processing was accomplished in three steps. First, a smooth background was removed from each raw diffractogram using a cubic spline function defined by points with $2\theta < 10°$ and $2\theta > 60°$. Secondly, the diffraction pattern from a non-crystalline sample of the same composition was scaled and subtracted from the semicrystalline pattern. The residual pattern represents the crystalline component of the original diffractogram. The crystallinity index is defined as the ratio of the area under the residual pattern divided by the total scattering in the original pattern (see ref. 23). Reflection positions were defined by deconvoluting the residual pattern into a series of Gaussian peaks.

Differential scanning calorimetry. Two different thermal analysis stations were used: a Du Pont 990 DSC to measure most thermal scans, and a Perkin–Elmer DSC7 to study the crystallization kinetics and scanning rate effect (2 to 150°C min^{-1}). All samples were equilibrated at about 10°C above their equilibrium melting temperatures for 10 min prior to measurements. The d.s.c. heating rate was 10°C min^{-1}, unless otherwise specified. All thermal scans were conducted under nitrogen. For the crystallization kinetics study, the specimens were cooled at a rate of 320°C min^{-1} from the temperature of an equilibrated melt state to the desired temperature. The isothermal crystallization peak time was recorded to characterize the crystallization rate.

Microscopy and optical techniques. The electron microscopy work was carried out on a JEOL 2000FX transmission instrument. Images were obtained at 100 kV accelerating voltage and recorded on film. The optical microscope used was a polarizing Nikon Optiphot-PDL model equipped with a 35 mm camera and a Mettler FP82 HT hot stage. A first-order red tint plate was used to determine the birefringent sign of the spherulite under crossed polars. The small-angle light scattering apparatus included a He–Ne unpolarized laser, two polarizers and a Polaroid 55 camera, and was used to characterize the spherulite dimensions and also the birefringent sign of the spherulite.

Table 2 The polymer 'diad' distribution in PEKK

T/I ratio	TT/TI
100/0	100/0
80/20	60/40
70/30	40/60
60/40	20/80
50/50	0/100

RESULTS

X-ray diffraction

Melt-crystallized PEKK. The powder diffraction of melt-crystallized PEKK(100/0) is shown in *Figure 2*. The diffraction pattern is similar to that of other all-*para* poly(aryl ether ketone)s. However, the reflections are shifted to lower angles because of the higher keto content.

The diffraction pattern can be indexed by a two-chain orthorhombic unit cell with dimensions $a = 0.769$ nm, $b = 0.606$ nm and fibre axis $c = 1.016$ nm (see *Figure 3*).

Effect of I on the crystalline phase. Figure 4a shows the diffraction patterns of melt-crystallized PEKK with six different T/I ratios (100/0, 90/10, 80/20, 70/30, 60/40, 50/50). The reflection positions are unaffected by the change in polymer composition, indicating that the

Figure 3 Unit-cell parameters of poly(aryl ether ketone)s vs. keto content

unit-cell parameters are unchanged. There is, however, a change in the intensity of the 1 1 1 reflection ($2\theta = 20.6°$) (with respect to the 1 1 0 reflection ($2\theta = 18.5°$)) with increasing isophthalate content.

Since PEKK(100/0) and (50/50) are homopolymers, the 1 1 1/1 1 0 intensity ratio in their respective diffraction patterns represents the extremes of total inclusion (50/50) into and total exclusion (100/0) of I from the crystalline phase. For intermediate compositions, if both T and I are included in the crystal without prejudice then a linear relationship should exist between the 1 1 1/1 1 0 intensity ratio and percentage of T (full line in *Figure 5a*). Deviations from a linear relationship would suggest some degree of exclusion. Total exclusion would result in a step function similar to that indicated by the broken line in *Figure 5a*. The 1 1 1/1 1 0 intensity ratio is plotted in *Figure 5a* against the percentage of T. While PEKK(60/40) and (90/10) have intensity ratios consistent with inclusion, PEKK(80/20) and (70/30) have ratios well above the expected values, indicating that some I units are excluded from the bulk of the crystal. The data suggest that up to 20% of the 'wrong' diad can be incorporated into each structure. The general shape of the intensity relationship leads us to conclude that the crystalline phase in PEKK(50/50) and (60/40) mainly consists of TI diads, while PEKK compositions with higher T content mainly consist of TT diads.
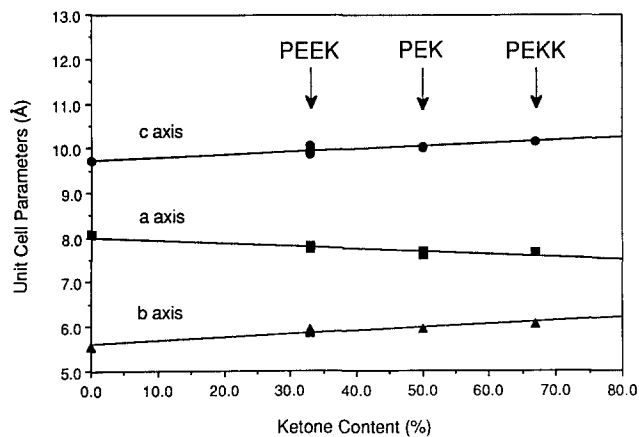

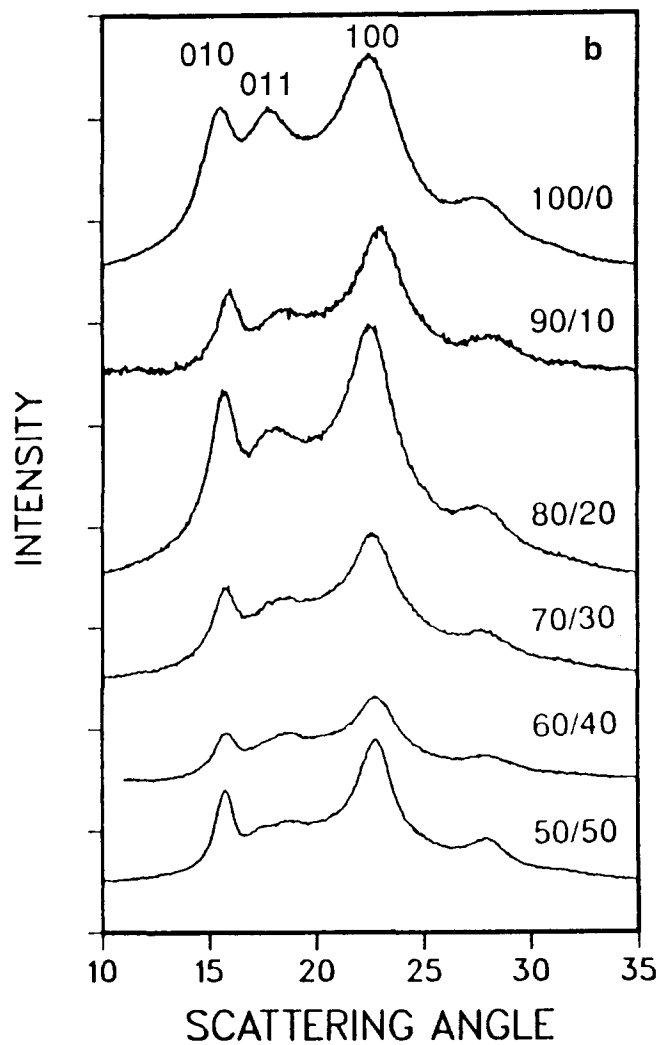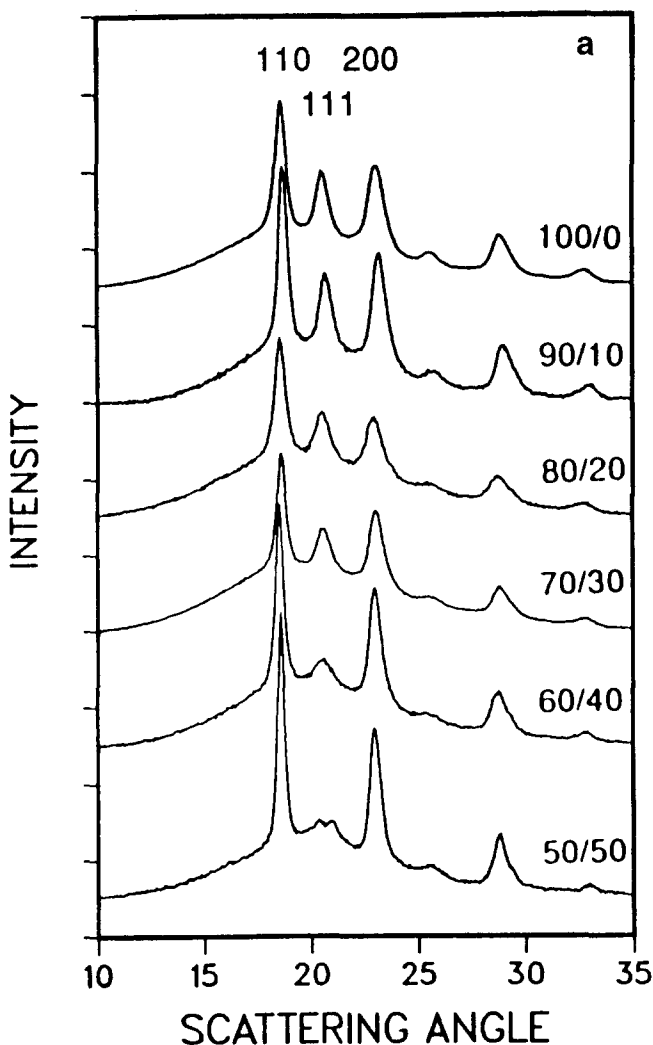**Figure 4** X-ray diffraction patterns of (a) melt-crystallized and (b) solvent-crystallized PEKK with different T/I ratios

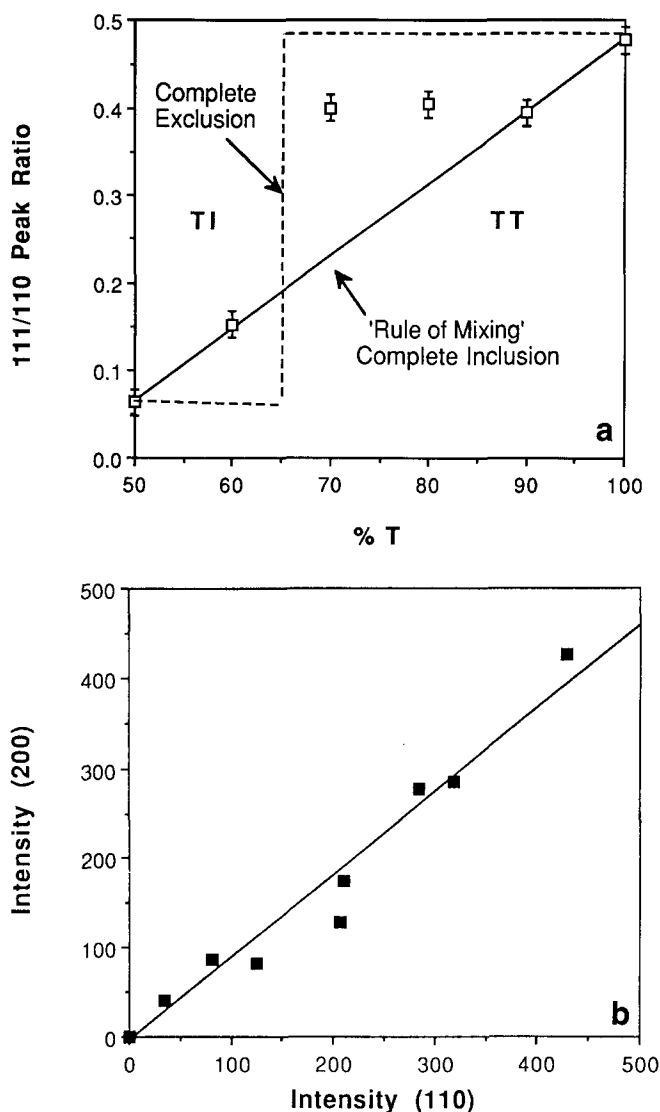reflection positions for form 2, like form 1, are relatively unaffected by the incorporation of isophthaloyl moieties.

Schematic diagrams of the chain packing modes for form 1 and form 2 that predict diffraction patterns consistent with those we observe are shown in *Figure 6*. Possible interchain interactions are limited to alignment of weak dipoles and phenyl–phenyl interactions. These phenyl–phenyl interactions are edge-to-face in form 1, but face-to-face in form 2.

The diffraction patterns of non-crystalline, quenched, PEKK samples that have been heat treated at 200°C show that both form 1 and form 2 are present[22,23]. The transition temperature of the different crystalline phases and their dependence on T/I composition are discussed below.

Melting and crystallization behaviour

Figure 7 reports the X-ray diffraction patterns and d.s.c. traces for PEKK(50/50) specimens prepared by melt crystallization and cold crystallization at 200°C. The X-ray diffraction patterns show that cold crystallization produces a mixture of form 1 and form 2, while the melt crystallization produces only form 1. The difference between the two d.s.c. scans indicates that the endotherm at about 280°C is associated with the melting of form 2 while the endotherms at about 300 and 330°C are associated with the melting of form 1. Both d.s.c. scans exhibit a small endotherm at about 220°C. This peak is attributed to double-melting behaviour and will be discussed later.

Different preparation protocols produce different morphologies. For example, the d.s.c. scan of a solvent-crystallized PEKK(50/50) specimen having only the form 2 structure is shown in *Figure 8* (top curve). This scan is similar to that of a cold-crystallized specimen in *Figure 7*, but some differences can be found: a sharp exotherm appears at 290°C and a small endothermic peak at 220°C disappears. The sharp exotherm at 290°C might be associated with the conversion (at least partial) of form 2 to form 1. In the d.s.c. scan of a quenched, amorphous specimen (second curve) an exotherm at 225°C appears. This exotherm is attributed to the cold crystallization, which produces a mixture of form 1 and form 2 as discussed previously. The d.s.c. scan of a slow cooled PEKK(50/50) specimen (third curve) differs from the previous two. The 280°C peak is completely eliminated and replaced by two peaks at 300 and 330°C. The X-ray pattern shows that this specimen contains only form 1 structure; therefore, these two peaks are related
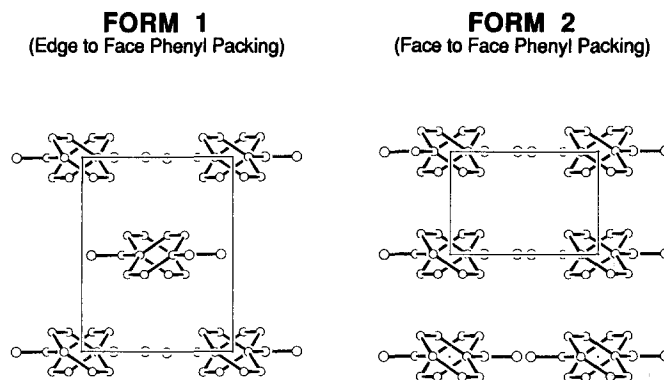

Figure 5 Plots of (a) the 1 1 1/1 1 0 peak ratios vs. percentage of T and (b) the intensity of the 2 0 0 reflection vs. the intensity of the 1 1 0 reflection for melt-crystallized PEKK samples

The intensity of the 2 0 0 reflection is plotted against the intensity of the 1 1 0 reflection for different T/I ratios in *Figure 5b*. The linear correlation between the intensities of these two equatorial reflections indicates that the TT and TI structures look the same in projection down the chain axis.

Solvent-crystallized and cold-crystallized PEKK. PEKK can also be crystallized by exposing quenched noncrystalline films to methylene chloride. The diffractometry scans of the six T/I compositions of solvent-crystallized PEKK are shown in *Figure 4b*. All of the patterns show a new reflection at ca. $2\theta = 15.6°$ that is not observed in melt-crystallized materials. The simplest explanation for this reflection is that it is the 0 1 0 reflection of a one-chain (metrically) orthorhombic unit cell ($a = 0.393$ nm, $b = 0.575$ nm and $c = 1.016$ nm) that has been designated as form 2. Attempts were made to improve the crystallinity and perfection of this crystalline phase by thermal treatments, and some improvement has been achieved. However, high-temperature annealing produces a conversion to a structure indistinguishable from that of melt-crystallized material (form 1). The

FORM 1
(Edge to Face Phenyl Packing)

FORM 2
(Face to Face Phenyl Packing)

Figure 6 Schematic drawing of chain packing modes in form 1 and form 2
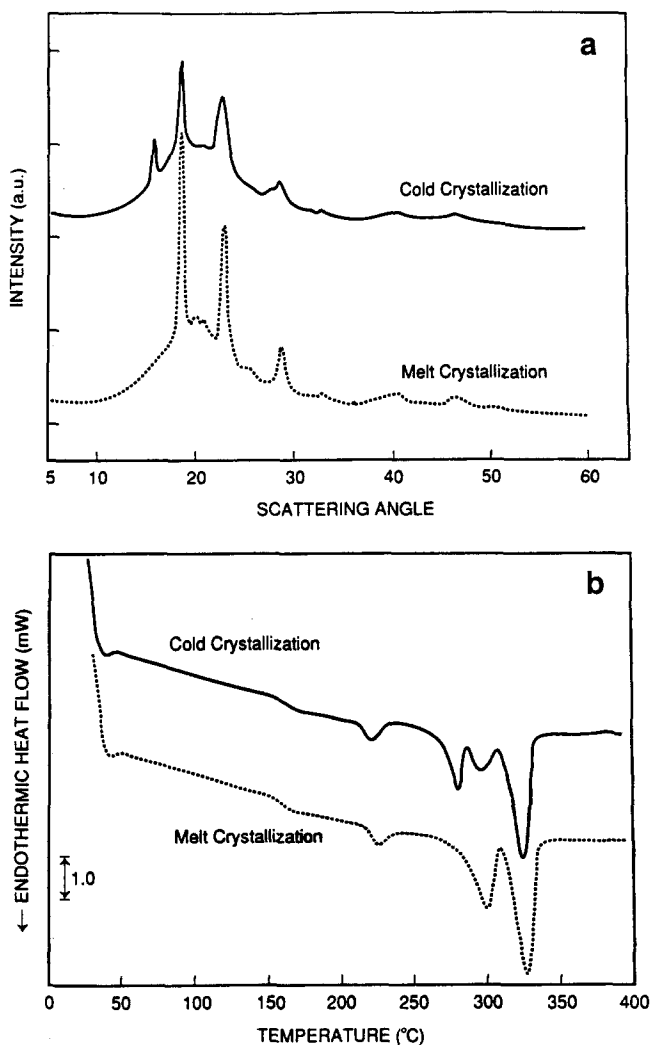
Figure 7 (a) X-ray diffraction and (b) d.s.c. scans of PEKK(50/50) specimens having different crystal forms. Both melt-crystallized and cold-crystallized specimens were held at 200°C for 6 h

to the melting of form 1. Finally, annealing at 270°C (bottom curve) produces a small endotherm at 280°C. This is not due to the melting of form 2 (verified by the X-ray diffraction). It has always been observed that an endotherm occurs about 10°C above the isothermal annealing temperature. Such behaviour is called the double-melting behaviour and has been seen in PEEK and other semicrystalline polymers[14,17,18,29]. Although the exact cause is not yet proven, there is increasing evidence that this peak is associated with the melting of a secondary structure within the spherulite[17,30].

Figures 9a–c show d.s.c. traces of PEKK(90/10), (80/20) and (70/30), respectively, annealed at several temperatures for 30 min. The d.s.c. traces of PEKK(60/40) and (50/50) annealed at several temperatures for 1 h are shown in *Figures 10a* and *10b*. It is apparent that PEKK(90/10), (80/20) and (70/30) show the straightforward double-melting behaviour while PEKK(60/40) and (50/50) melt in a more complicated manner with an additional high-temperature peak at about 330°C. Among these samples, (50/50) has the most complicated melting behaviour. This is rationalized by the following argument. The addition of isophthalate units increases the chain flexibility (see discussion), but PEKK(50/50) is also a homopolymer while the rest are random

copolymers. Therefore, (50/50) consists of not only the highest chain flexibility but also the highest chain regularity among the five specimens containing isophthalate residues. These two factors may inevitably complicate the crystallization and melting behaviour.

We have studied the effect of d.s.c. scanning rate on the thermal behaviour of the annealed (50/50) and (60/40) specimens. The results are shown in *Figures 11a* and *11b*. It is noted that the annealing-induced low-temperature peak and the middle endotherm are invariant in magnitude for all heating rates and, therefore, are due to the melting of two thermodynamically (meta)stable states. In contrast, the size of the high-temperature peak does depend on the heating rate. At rates larger than $100°C\ min^{-1}$, this peak is completely eliminated, suggesting that this transition may be due to a recrystallization or reorganization process. The middle peak (at about 310°C), therefore, represents the melting of form 1. We have interpreted this peak to signal the nominal melting temperature. Hoffman–Weeks plots using the melting temperatures retrieved from *Figures 9* and *10* are shown in *Figure 12*. The equilibrium melting temperature is extrapolated from the interception of the broken line and the $T_m = T_c$ line. It is clear that the increase of isophthalate content decreases the equilibrium melting temperature. We have plotted the equilibrium melting temperature vs. the terephthalate content, which shows a linear relationship (*Figure 13*).

Another interesting aspect of the crystallization is the crystallization kinetics. This is studied by the isothermal d.s.c. crystallization half-time method. However, it is difficult to measure the half-time if the crystallization rate is fast. An alternative method is to study the crystallization peak time (time that has a maximum heat flow), as shown in *Figure 14*. We find that the crystallization rate increases with decreasing isophthalate content, except for (50/50), which crystallizes faster than (60/40). A difference in crystallization behaviour is observed for TI structures, (50/50) and (60/40), *versus* TT structures with exclusion, (70/30) and (80/20), *versus* TT structures with inclusion, (90/10) and (100/0).
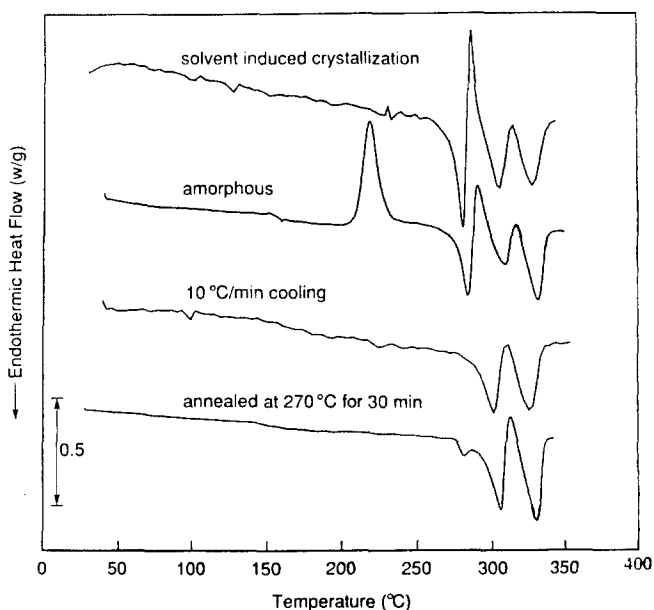

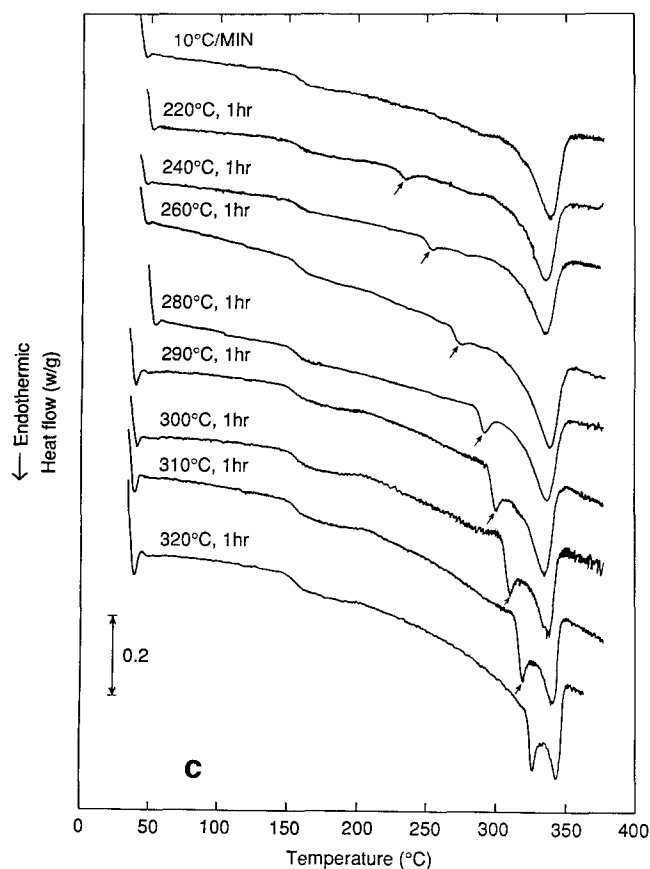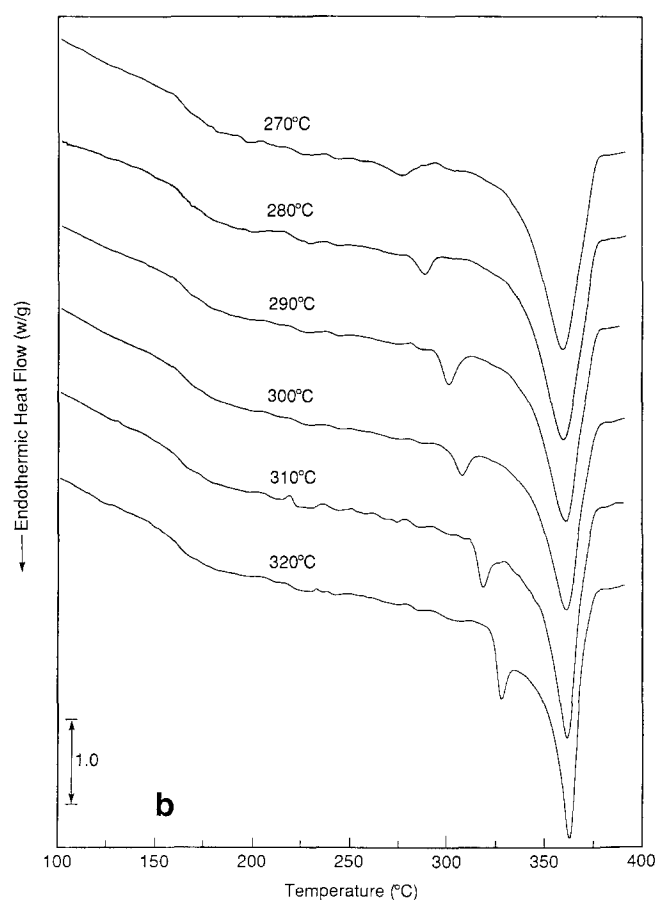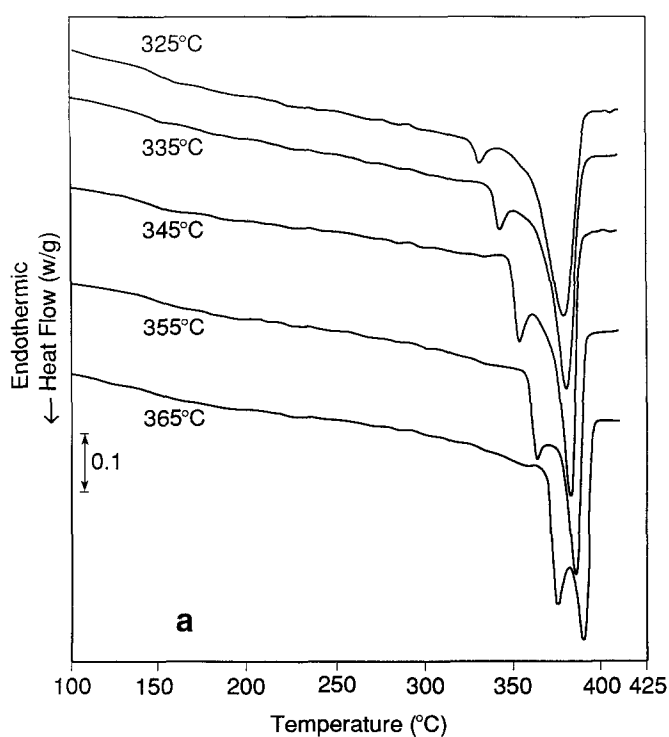**Figure 8** D.s.c. scans of four different PEKK(50/50) specimens. The treatment conditions are as specified

Figure 9 D.s.c. scans of PEKK specimens annealed at different temperatures for 30 min: (a) PEKK(90/10), (b) PEKK(80/20), (c) PEKK(70/30)

along the 45° azimuthal angle; the V_V scattering shows a vertical two-fold symmetric pattern. The vertical V_V pattern suggests that the anisotropy of polarizability is tangential within the spherulite, which is a clear indication of the negative sign of birefringence. Since the anisotropy of polarizability of PEKK chains is positive ($a_c > a_b$), the unit-cell c axis must lie along the tangential direction of the spherulite and the b axis must be parallel to the radial (or growth) direction.

A TEM image of an etched melt-crystallized PEKK specimen surface (*Figure 15b*) shows a sheaf-like spherulitic structure having fine lamellar features. Such a structure is quite common in many crystalline polymers[34,35] and is certainly indistinguishable from that of PEEK[15,17]. The spherulite is initiated from a sheaf-like formation of lamellae and then develops by infilling growth. The etching technique has revealed fine lamellar details of the spherulite. In *Figure 15b*, stacks of lamellae with a periodicity of about 15 nm are clearly seen. This dimension is quite close to the long period determined by small-angle X-ray scattering, as will be discussed elsewhere.

Figures 17 and *18* show TEM images of replicas of the etched spherulite morphology of PEKK(60/40) and (70/30) having different thermal histories. *Figures 17a–c* are micrographs of (70/30) prepared under the following conditions: (a) fast cooled at 50°C min^{-1} rate, (b) slow cooled at 5°C min^{-1} rate and (c) annealed at 300°C for 30 min. In the case of fast cooling, the specimen is partially crystallized (about 20% crystallinity). *Figure*

Morphology

A typical optical micrograph of the melt-crystallized PEKK spherulites is shown in *Figure 15a*. These spherulites are all negatively birefringent as identified by a polarizing optical microscope equipped with a quarter-wave plate[31] and a small-angle light scattering device[32,33]. The small-angle light scattering patterns (V_V and H_V) are shown in *Figure 16*. The H_V scattering shows a four-leaf-clover pattern with the maximum intensity
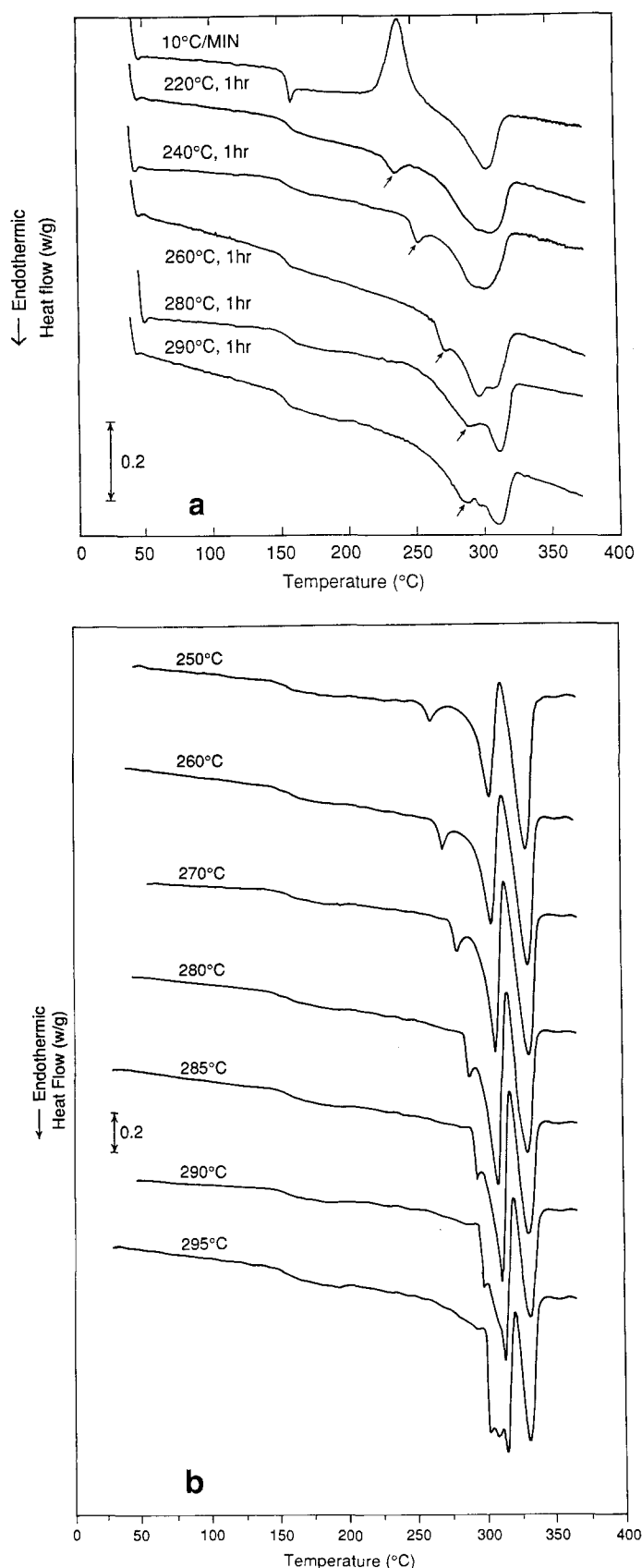
poorly defined, possibly because the predominant amorphous material was eaten away during the etching, leaving behind the initial crystalline structure. The TEM images in *Figures 17b* and *17c* are quite different from that in *Figure 17a*, which has only broad, indistinct lamellar layers. However, *Figures 17b* and *17c* differ from each other in the appearance of impinging spherulite boundaries. *Figure 17b* shows relatively diffuse boundaries and *Figure 17c* shows distinct straight boundaries. This difference is even more dramatic in *Figures 18a* and *18b*, where TEM images of (60/40) under two different thermal treatments are shown. These treatments included: (a) a slow cooling at $2°C \, min^{-1}$ rate and (b) an annealing at 260°C for an hour. The slow-cooled specimen (*Figure 18a*) reveals a distinct lamellar structure, whereas the annealed specimen shows a broad and indistinct one.

DISCUSSION

X-ray diffraction studies[1-4,7-11] support the following generalizations: (1) Regardless of chemical structure, poly(aryl ether ketone)s appear to pack into a two-chain orthorhombic unit cell with two phenyl groups (and two linkage groups) in the crystallographic repeat. (2) The chains are arranged at the corner and centre of the unit cell, $(0, 0, Z)$ and $(\frac{1}{2}, \frac{1}{2}, Z')$. (3) The chains adopt a fully extended conformation and have adjacent phenylene groups rotated out of the plane of the linkage groups by the angle $\pm \gamma$, where γ varies from 30 to 50°. (4) The apparent space group, *Pbcn* (no. 60), requires that all of the phenyl groups and all of the linkage groups be *symmetrically related and therefore identical*.

There are two possible explanations for the observation of a crystallographic repeat that is shorter than the chemical repeat and for the super-symmetry. First, the observed cell could be a sub-cell of the true unit cell, i.e. the electron density difference between the ether and keto groups is so small that reflections corresponding to the true repeat are not observed. If this is the correct model, the keto linkages are expected to be segregated from the ether linkages. The second model is one in which the chains are randomly shifted past each other. The result of such a shift would produce a 'non-segregated' structure with ether groups packing adjacent to keto groups and vice versa. This model would lead to the observation of an 'averaged' two-phenyl crystallographic repeat where a given linkage could lie at any linkage site in the crystal. In both models the 'average' linkage group depends on the polymer composition. Indeed, *Figure 2* displays a plot of the unit-cell parameters *versus* the keto content in the 'average' linkage for different poly(aryl ether ketone) structures taken from the literature[1-4,7-11,36]. There is a single, simple linear dependence of the cell parameters on the keto content. The c and b cell parameters increase with increasing keto content, the former because of the increased stiffness of the keto group and the latter because of the keto group's larger bulk. The third parameter, a, decreases to preserve the density of the system.

This study has investigated the effect of incorporating *meta* linkages (via isophthaloyl moieties) on the structure and crystallization of the particular family member denoted PEKK. It was found for all T/I ratios that melt-crystallized PEKKs form a structure similar to other poly(aryl ether ketone)s, i.e. form 1. However, a clear difference is seen between compositions with high and
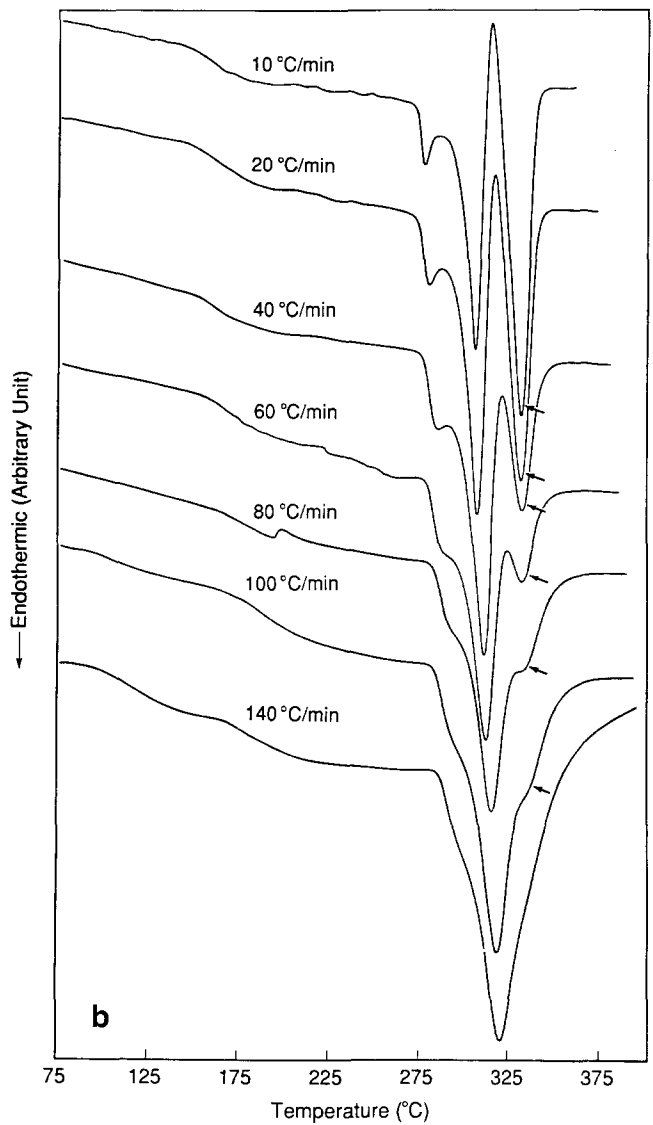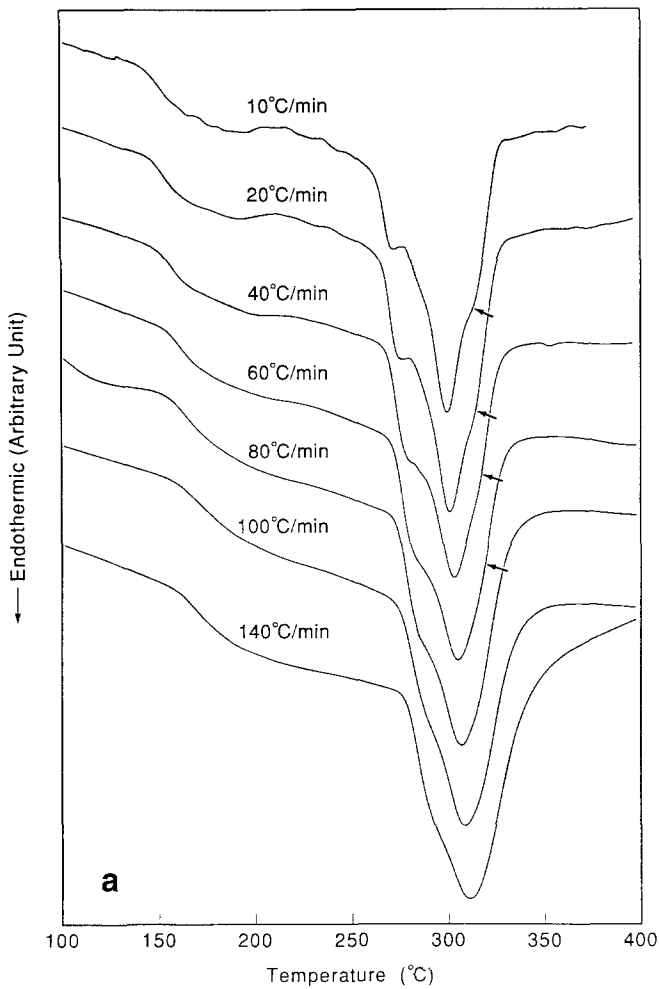
Figure 10 D.s.c. scans of PEKK specimens annealed at different temperatures for 1 h: (a) PEKK(60/40), (b) PEKK(50/50)

17a thus represents the structure developed during the early stage of crystal growth (or the primary crystallization stage). The sheaf-like skeleton lamellar formation is seen, which has often been found in the early stage of PEEK spherulite growth[12,13,15,17]. The lamellae are

Figure 11 (a) D.s.c. scans of an annealed PEKK(60/40) specimen (held at 260°C for 60 min) at different heating rates. (b) D.s.c. scans of an annealed PEKK(50/50) specimen (held at 270°C for 60 min) at different heating rates
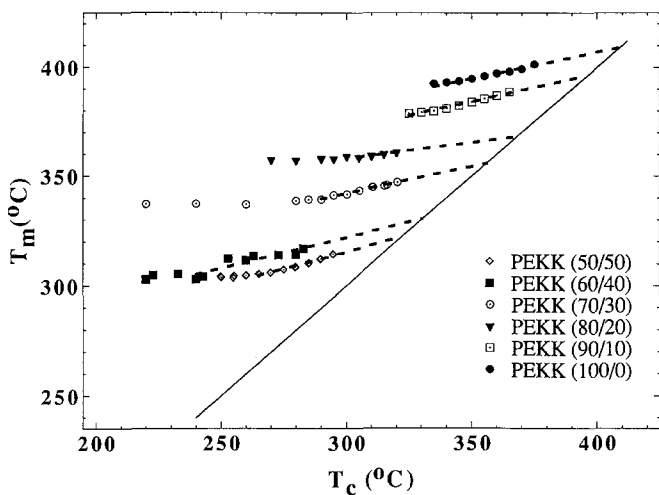

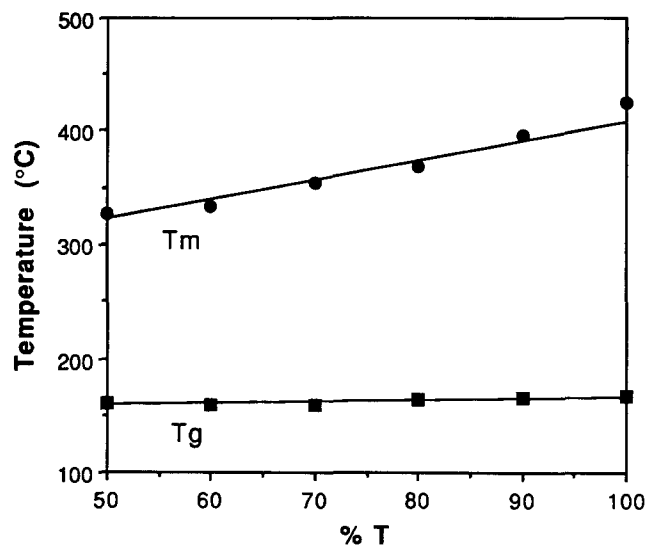**Figure 12** The Hoffman–Weeks plot of PEKKs having six different T/I ratios

Figure 13 The extrapolated equilibrium melting temperature and glass transition temperatures vs. T content

low isophthalate content. PEKKs containing ≤30% isophthalate content pack in a structure that consists mainly of TT diads. In contrast, PEKKs containing 40 and 50% isophthalate consist of TI diads.

The rate-dependent high melting peak that is observed in samples containing TI crystals (at 330°C, as seen in

Figure 11b) is associated with a recrystallization or reorganization process. This behaviour can be explained by the increase of chain flexibility in PEKK(50/50), which may result in rearranging the crystal structure to a more perfect one after premelting. We suspect that this
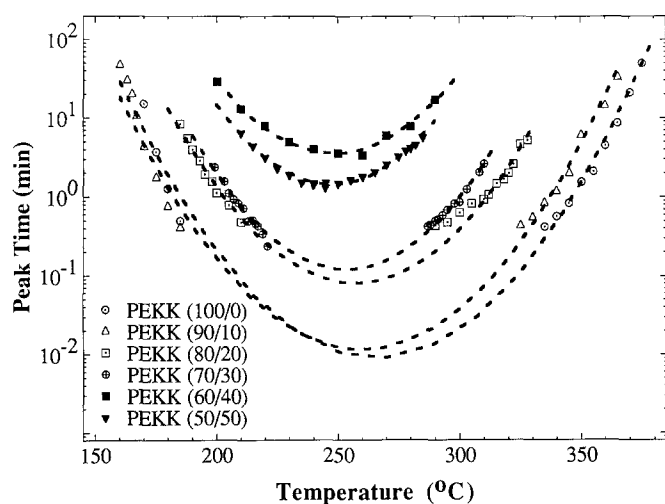
Figure 14 Plot of crystallization peak time vs. temperature for six different PEKKs
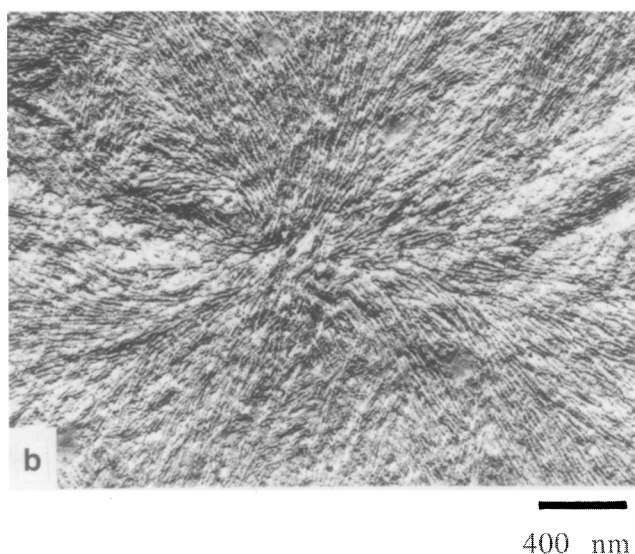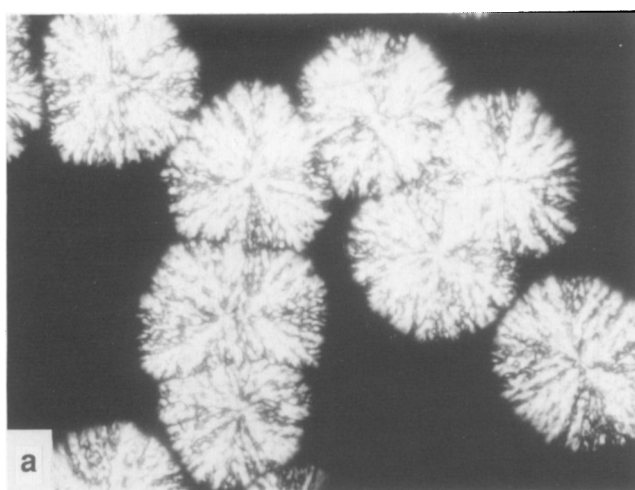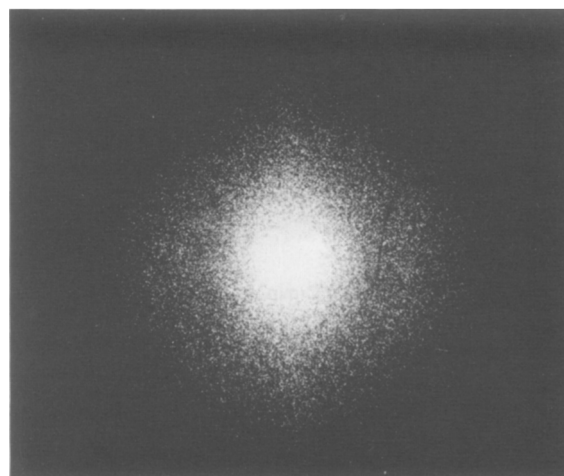

10 μm

400 nm

Figure 15 Two micrographs of the PEKK spherulite: (a) a polarized optical microscopic image and (b) a TEM image of a replica surface. The specimen is a PEKK(60/40) sample annealed at 280°C for about 30 min
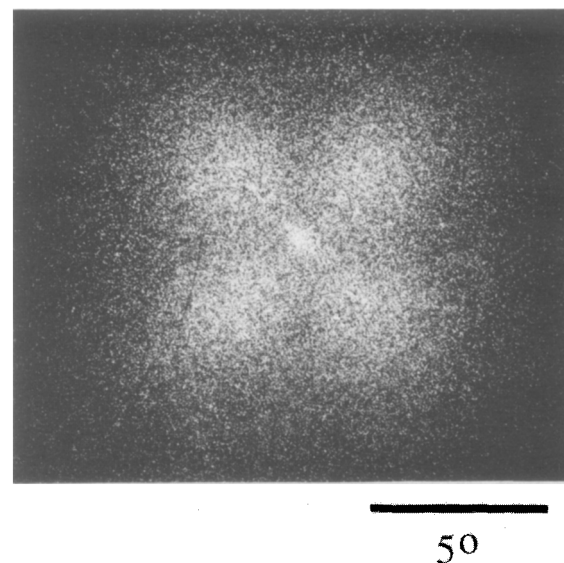

Figure 16 Small-angle light scattering patterns (V_V and H_V) of a crystallized PEKK(70/30) specimen

transition corresponds to the conversion of a structure containing random shifts of the chains past each other to a structure where the isophthalate groups are segregated. *Figure 19* shows the local conformation about a terephthalate group and two possible conformations about an isophthalate group. The two 'isophthalate' conformations differ in the relative rotations of the phenyl rings on each side of the isophthalate unit. It is clear that the overall shape and therefore potential packing interaction is different for the two phthaloyl moieties. Consequently, the presence of the isophthalate moiety in the crystal can be viewed as a symmetry or entropic defect.

It is conceivable that, upon annealing or premelting, these defects can segregate to produce a more stable state. However, our evidence is not conclusive. Further experiments, including neutron scattering, are planned to probe this possiblity. In general, the incorporation of *meta* isomers affects two aspects of the crystallization in PEKK. First, it introduces a symmetry (or entropy) defect in the chain within the crystal unit cell, as we have inferred from the crystallographic data. Secondly, it increases the chain flexibility in the melt. An increase of chain flexibility can be inferred by the observation that
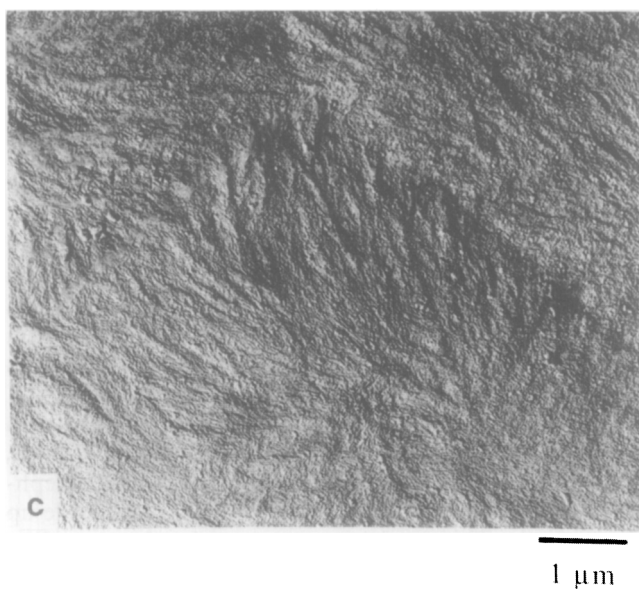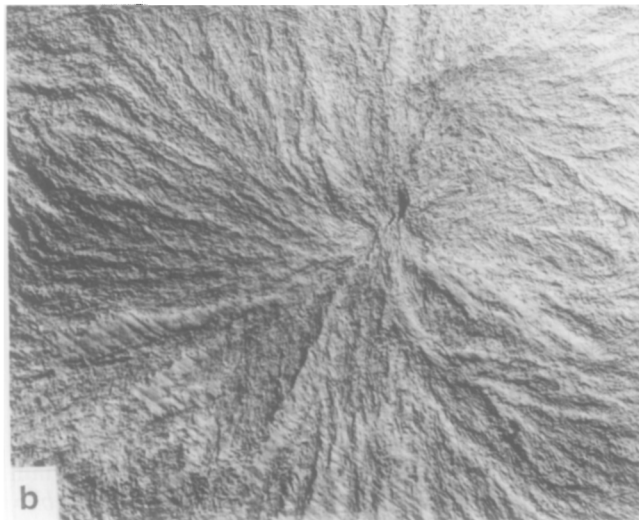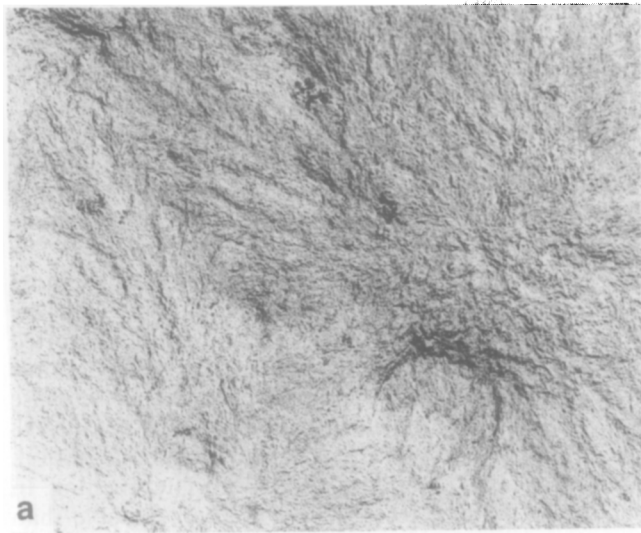
5 µm

Figure 18 TEM micrographs of replica surfaces of etched PEKK(60/40) specimens. Samples were prepared under: (a) slow cooling (5°C min⁻¹) and (b) annealing at 260°C for 30 min

1 µm

Figure 17 TEM micrographs of replica surfaces of etched PEKK(70/30) specimens. Samples were prepared under different treatments: (a) fast cooling (50°C min⁻¹), (b) slow cooling (5°C min⁻¹) and (c) annealing at 300°C for 30 min
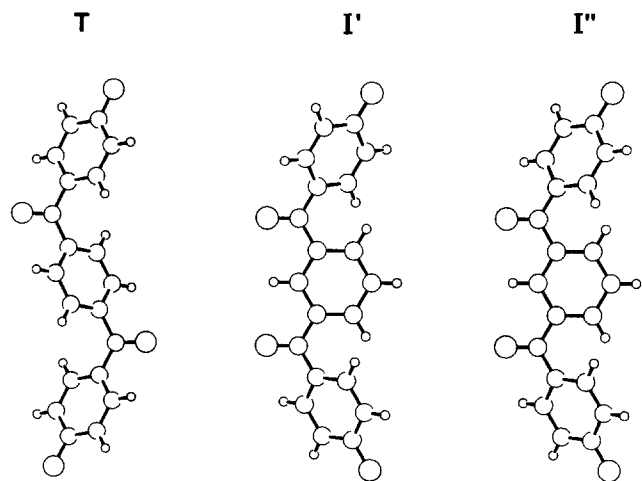

Figure 19 Molecular configuration of PEKK chains having I isomers in the crystalline phase

the increase of *meta* isomer content decreases the glass transition temperature (*Figure 13*; PEKK(100/0) T_g = 165°C, PEKK(50/50) T_g = 155°C). The crystallization rate is also affected by chain flexibility. As the *meta* isomer content decreases, the chain becomes stiffer and the crystallization rate generally increases. If we compare homopolymers, PEKK(100/0) crystallizes faster than PEKK(50/50). For copolymers, the crystallization rate increases in the order (60/40) < (70/30) ≈ (80/20) < (90/10).

The molar heat of fusion for the *meta* and *para* isomers are about the same, since there is no difference between the maximum heat of fusion for the low and high T/I ratio PEKKs. The comparable heats of fusion and the diffraction data suggest that neither the exclusion model nor the inclusion model[38] for predicting the copolymer melting point is appropriate for describing the melting-point depression in PEKK. The PEKK copolymers appear to behave in a manner intermediate between the extreme assumptions of the two theories, i.e. both components (*para* and *meta*) are capable of crystallizing with the same heat of fusion, but have different entropy change during crystallization.

The annealing-induced endotherm in the d.s.c. thermogram has been attributed to the melting of a secondary structure within the spherulite. This was studied by the thermal, optical and small-angle light scattering methods, which showed that, after the first melting (annealing-induced endotherm), the spherulite size remained constant but the integrated transmitted light intensity decreased. The integrated transmitted light intensity is partially associated with the total degree of crystalline ordering within the spherulite. Therefore, the decrease of intensity indicates that the ordering within the spherulite may be reduced. In addition, the secondary crystallization consists of crystallization from two different aspects: one contributes to the crystal perfection such as lamellar thickening; and another one contributes to the crystal imperfection such as lamellar subsidiary branching and low-molar-mass crystallization. The melting of imperfect crystals certainly will occur at a low temperature and may produce an annealing-induced endotherm.

Our TEM work has revealed a difference between the microstructure of fast- and slow-cooled PEKK specimens. Structure was developed during the initial primary crystallization stage, which showed only a single endotherm in the d.s.c. scan. This endotherm occurred at a high temperature, which indicates that the primary structure consists of more perfect crystals. We have also noticed that the primary structure has a less defined lamellar feature than that of a slow-cooled or annealed specimen. This is because the specimens do not undergo a lamellar thickening process during fast cooling but they have ample time to thicken the lamellae during slow cooling. In the case of PEKK(80/20) or (50/50), the melt-crystallized specimen shows a similar spherulite structure, at least by optical techniques. The morphological appearance is not a direct function of the isophthalate content but depends strongly on the thermal history and the corresponding crystallization rate. Finally, our observation of the different spherulitic boundary morphology is possibly associated with the diffusion process of the low-molar-mass components and/or impurities during crystallization. In the isothermal crystallization, these components may be excluded from the

spherulite and segregated to the boundaries, leaving a distinct boundary morphology after etching. In the non-isothermal crystallization, they may be trapped within the spherulite, leaving behind diffuse boundaries.

In contrast to the rest of the poly(aryl ether ketone) family, PEKK specimens, regardless of T/I ratio, can be induced to show a second crystalline modification, form 2, either by solvents or cold crystallization. We attribute its existence to the high keto content in PEKKs. The two packing modes for PEKK are similar to those observed in the aromatic polyamide, poly(*p*-phenylene terephthalamide)[37]. (Blundell[27] has recently reported the observation on a 'new' structure for PEKK. While indexed differently, his structure corresponds to the phase we have labelled form 2.) In the case of PEKK(50/50), form 2 has a lower melting temperature (about 280°C), and may be able to convert into form 1 after melting. In this case, form 2 is thermodynamically less stable than form 1 and requires less mobility to form.

CONCLUSIONS

Many PEKK characteristics can be understood as typical of the family of poly(aryl ether ketone)s, e.g. form 1 structure, T_g and T_m. We have investigated the crystallization, melting and morphology of PEKK having different *para/meta* isomer ratios. In contrast to related poly(aryl ether ketone)s, PEKK has two different crystal structures: a conventional form 1 structure, the same as that observed in PEEK and PEK, which is usually developed from melt crystallization, and a new form 2 structure, which can be developed from solvent crystallization or cold crystallization. Form 1 has a two-chain orthorhombic unit cell (a = 0.769 nm, b = 0.606 nm and fibre axis c = 1.016 nm) while form 2 has a one-chain (metrically) orthorhombic unit cell (a = 0.786 nm, b = 0.575 nm and c = 1.016 nm). The form 2 structure is capable of converting into form 1 after melting.

The addition of the *meta* isomer (isophthalate moiety) decreases the equilibrium melting temperature and the crystallization rate, but increases the chain flexibility and the recrystallization ability. It has little effect on the unit-cell dimensions and the entropy of fusion or the total degree of crystallinity. In fact, in the unit cell, the terephthalate and isophthalate groups are crystallographically isomorphous. The *meta* linkage can be viewed as creating 'symmetry or entropy defects' in the unit cell and these defects are responsible for the equilibrium melting-temperature depression. The extent of correlation between these defects (if any) cannot yet be quantified. It may depend on crystallization kinetics. The correlation can be probed by neutron scattering of PEKK specimens having the isophthalate segment deuterated.

The diffraction data indicate that compositions with high isophthaloyl content, PEKK(50/50) and (60/40), consist of TI diads and compositions with high terephthaloyl content, PEKK(70/30) to (100/0), are made up of TT diads. This model is supported by the crystallization data. The d.s.c. scans show a double-melting behaviour for TT crystals (*Figure 9*) and a triple-melting behaviour for TI crystals (*Figure 10*). In addition, the crystallization rate is very different for TT and TI crystals (*Figure 14*).

REFERENCES

1   Radhakrishnan, S. and Nadkarni, V. W. *Polym. J. Mater.* 1985, **2**, 93
2   Dawson, P. C. and Blundell, D. J. *Polymer* 1980, **21**, 577
3   Fratini, A. V., Cross, E. M., Whitaker, R. B. and Adams, W. W. *Polymer* 1986, **27**, 861
4   Hay, J. N. and Kemmish, D. J. *Polym. Commun.* 1989, **30**, 77
5   Abraham, R. J. and Haworth, I. S. *Polymer* 1991, **32**, 121
6   Jog, J. P. and Nadkarni, V. M. *J. Appl. Polym. Sci.* 1986, **32**, 3317
7   Rueda, D. R., Ania, F., Richardson, A., Ward, I. M. and Balta Calleja, F. J. *Polym. Commun.* 1983, **24**, 258
8   Wakelyn, N. T. *Polym. Commun.* 1984, **25**, 306
9   Yoda, O. *Polym. Commun.* 1984, **25**, 238
10   Hay, J. N., Kemmish, D. J., Langford, J. I. and Rae, A. I. M. *Polym. Commun.* 1984, **25**, 175
11   Hay, J. N., Kemmish, D. J., Langford, J. I. and Rae, A. I. M. *Polym. Commun.* 1985, **26**, 283
12   Lovinger, A. and Davis, D. D. *Macromolecules* 1986, **19**, 1861
13   Lovinger, A. and Davis, D. D. *J. Appl. Phys.* 1985, **58**, 2843
14   Blundell, D. J. and Osborn, B. N. *Polymer* 1983, **24**, 953
15   Olley, R. H., Bassett, D. C. and Blundell, D. J. *Polymer* 1986, **27**, 344
16   Kumar, S., Anderson, D. P. and Adams, W. W. *Polymer* 1986, **27**, 329
17   Bassett, D. C., Olley, R. H. and Al Raheil, I. A. M. *Polymer* 1988, **29**, 1745
18   Chang, S. Z. D., Cao, M. Y. and Wunderlich, B. *Macromolecules* 1986, **19**, 1868
19   Mensitieri, G., Del Nobile, M., Apicella, A., Nicolais, L. and Garbassi, F. *J. Mater. Sci.* 1990, **25**, 2963
20   Grayson, M. and Wolf, C. *J. Polym. Sci., Polym. Chem. Edn.* 1987, **25**, 31
21   Stober, E. J., Seferis, J. C. and Keenan, J. D. *Polymer* 1984, **25**, 1945
22   Matheson, R. R., Chia, Y. T., Avakian, P. and Gardner, K. H. *ACS Polym. Prepr.* 1988, **29**, 468
23   Avakian, P., Gardner, K. H. and Matheson, R. R. *J. Polym. Sci., Polym. Lett. Edn.* 1990, **28**, 243
24   Chang, I. Y. *SAMPE Q.* 1988, **19**, 29
25   Sauer, B. B., Avakian, P., Starkweather, H. and Hsiao, B. S. *Macromolecules* 1990, **23**, 5119
26   Hsiao, B. S., Chang, I. Y. and Sauer, B. B. *Polymer* 1991, **32**, 2799
27   Blundell, D. J. and Newton, A. B. *Polymer* 1991, **32**, 308
28   Gohil, R. M. and Phillips, P. J. *Polymer* 1986, **27**, 1687
29   Lee, Y. and Porter, R. S. *Macromolecules* 1988, **21**, 2770
30   Marand, H. personal communications, 1990
31   Meeten, G. H. 'Optical Properties of Polymers', Elsevier Applied Science, New York, 1986
32   Stein, R. S. and Rhodes, M. B. *J. Appl. Phys.* 1960, **31**, 1873
33   Samuels, R. *J. Polym. Sci. (A-2)* 1971, **9**, 2165
34   Wunderlich, B. 'Macromolecular Physics', Academic Press, New York, 1976, Vol. 2
35   Bassett, D. C. 'Principles of Polymer Morphology', Cambridge University Press, Cambridge, 1981
36   Boon, J. and Magre, E. P. *Makromol. Chem.* 1969, **126**, 130
37   Flory, P. J. *Trans. Faraday Soc.* 1955, **51**, 848
38   Sanchez, I. C. and Eby, R. K. *J. Res. NBS* 1973, **77**, 353